

The nlogistic-sigmoid function

Oluwasegun A. Somefun¹ Kayode Akingbade² and Folasade Dahunsi¹

Abstract—The variants of sigmoid functions used in artificial neural networks are, by definition, limited by vanishing gradients. Defining the sigmoid function to become n -times repeated over a finite input-output map can significantly reduce the presence of this limitation. This function mapping as proposed in this paper is the nlogistic-sigmoid function.

Index Terms—Activation Functions; Vanishing Gradients; Nonlinear Functions; Neural Networks.

I. INTRODUCTION

ACTIVATION functions (AFs) follow the basis that neurons in the brain are input-output dynamic systems [1]. The choice of such computational transfer-function mappings is of critical importance in the design of any artificial neural network (ANN) architecture, with significant control over the network's deep pattern learning ability or performance [2]–[4]. Logistic-sigmoid functions such as the simple logistic-sigmoid function (1) and the hyperbolic-tangent function (2) are common sigmoid-variant activation functions used in ANNs. It can be argued that sigmoid functions are popular, partly due to the fact that their derivatives make them compatible with gradient-descent algorithms [5], [6]. In addition, they are known to possess inherent output boundedness, continuously-differentiable $C^\infty(\mathbb{R})$, smooth, monotonic and nonlinear properties [4], [7], [8].

$$y = \mathbf{f}(x) = 1/(1 + e^{-x}) \quad (1)$$

$$y = \mathbf{f}(x) = \tanh(x) = (2/(1 + e^{2x})) - 1 \quad (2)$$

Therefore, logistic-sigmoid functions have found application in diverse areas, such as in physics, statistics, neuroscience, computer graphics, signal processing, feedback control and robotics. For example, the logistic-sigmoid function is the most common describing nonlinear regression function [9] for the biological baroreflex feedback regulation system in humans and animals [10]. It is also a recurring shape in nature, commonly observed in the motion-profile of ant swarms [11]. Further, sigmoid functions have been used to model actuating behaviours of high gain nonlinear operational amplifiers (amplifiers with saturation) [12]–[14], which function as signal limiting or relay (switching) functions. It has also been used to achieve smooth path-planning for mobile robots [15].

Likewise, the literature on sigmoid activation functions is rich. Considerable research have been dedicated to the

application and improvement of sigmoid functions, see [16]–[21]. An efficient approximation scheme for the VLSI implementation of neural networks with the hyperbolic-tangent function was proposed in [22]. The function approximation capability of sigmoids have also been investigated in relatively recent works. [23] using a broad class of common AFs, explored the smooth function approximation ability of deep neural networks. They further classify AFs into two groups: piecewise linear (rectified linear-unit (ReLU) variants) and locally quadratic (sigmoid variants). Notably, for best function approximation and faster convergence, it has been suggested that sigmoid functions should be symmetric about the origin of the function's input-output map [3]. Further, in application to multi-path signal propagation, [24] showed that the optimum AF for vector equalization using recurrent neural networks (RNNs) can be realised as a sum of shifted hyperbolic tangent functions.

Nevertheless, two notable inherent drawbacks affect sigmoid functions. As the first short-coming: formulations of sigmoid functions possess a fundamental learning (optimization) disadvantage in which their derivatives exponentially approach zero, especially as the network becomes deeper. This famous problem defined as the vanishing (exponential decreasing) gradient problem was first formally treated in [25], leading to the gradient-based Long Short-Term Memory (LSTM) recurrent neural network (RNN). More recently, this problem was also considered in [26]. Several proposals to partially overcome this issue have been explored in the literature. Some of the work-around solutions, apart from LSTM networks, reviewed in [27] are: deep-belief networks, hessian-free optimisation, random-weight guessing and leverage of GPU-based computational power. Consequently, more research led to the proposals of different alternative activation functions such as in [26], [28]–[32]. A concise survey of these proposed AFs in order to reduce the effect of vanishing gradients can be found in [33]. On the contrary, a common problem with most of these alternative AFs is that they cause more noisy outputs [26].

The second short-coming lies in the computational expensive arithmetic, in form of the natural exponential term e^u . This is why among AFs, the attractive property of low computational complexity and fast computational speed makes ReLU function variants popular as default choices in many deep neural-network architectures. Notwithstanding, sigmoid variants still stand out as the choice in architectures such as RNNs [34], [35]. Fortunately, through computer arithmetic techniques of function approximation, reduced computational complexity can be realized in software within acceptable levels of accuracy [34], [36].

In this brief, contrasted with the above discussed approaches in the literature, we treat the first shortcoming: the vanishing

*This work was not supported by any organization

¹Oluwasegun Somefun, and Folasade Dahunsi are with the Department of Computer Engineering, Federal University of Technology Akure, PMB 704 Ondo, Nigeria oasomefun@futa.edu.ng, fmdahunsi@futa.edu.ng

²Kayode Akingbade is with the Department of Electrical and Electronics Engineering, Federal University of Technology Akure, PMB 704 Ondo, Nigeria kfakingbade@futa.edu.ng

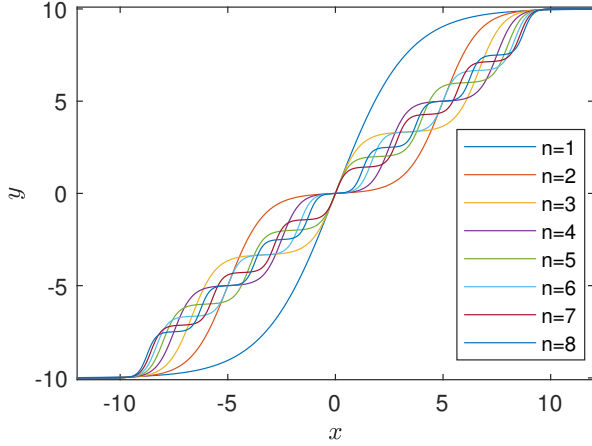


Fig. 1. Output Plot of the **n**logistic-sigmoid: $n = 1$ to 8.

gradient problem as a flaw in the logistic-sigmoid function definition. Specifically, for suitable use both as a activation and actuating function, we provide a more general and formal definition for such logistic-sigmoids over a finite input-output space. This is in form of the **n**logistic sigmoid function, illustrated in Fig. 1.

In section II, we start with a preliminary discussion on the classic sigmoid function. The proposed function is then defined in section III. It will be shown that by definition, the proposed function has over its input-output map, a n -times repeating gradient surface, with a maximum gradient of 3 which is a factor of 12 and 3 greater than (1) and (2) respectively. This implies that the proposed function can, to a large extent, reduce the vanishing occurrence of its gradients. Finally, in section IV, this paper is concluded. Useful for library developers, we provide an open-source implementation of this function in MATLAB and C/C++ [37].

II. CLASSIC LOGISTIC-SIGMOID

The classic logistic-sigmoid function given by (3) involve mapping a bounded output co-domain $y \in \mathbb{R}$ in the range $[y_{\min}, y_{\max}]$, where y_{\min}, y_{\max} are the minimum and maximum bounds or asymptotes of y respectively, to an unspecified or unbounded input domain $x \in \mathbb{R}$ in the range $(-\infty, \infty)$, centered by an offset parameter $\delta \in \mathbb{R}$, and scaled by a logistic growth-rate parameter $\alpha \in \mathbb{R}$.

$$y = \mathbf{f}(x) = y_{\min} + \frac{y_{\max} - y_{\min}}{1 + e^{\pm\alpha(x-\delta)}} \quad (3)$$

The derivative g with respect to the input is also given by (4). The maximum value of the derivative \bar{g} occurs at the inflection point (mid-point), where $x = \delta$. It can be easily shown that $\bar{g} \equiv 0.25\alpha(y_{\max} - y_{\min})$. At this point the corresponding value of y is $(y_{\max} + y_{\min})/2$.

$$g = \frac{dy}{dx} = \frac{\alpha}{y_{\max} - y_{\min}} (y - y_{\min})(y_{\max} - y) \quad (4)$$

For the simple logistic function (1), where $y_{\max} = 1$, $y_{\min} = 0$, $\alpha = 1$, and $\delta = 0$, we have $\bar{g} = 0.25$. On the other hand, for the hyperbolic tangent function (2), where $y_{\max} = 1$, $y_{\min} =$

-1 , $\alpha = 2$, and $\delta = 0$, we have $\bar{g} = 1$. These formulations are, therefore, limiting in the sense that the maximum gradient is both small and that the gradient exponentially decreases to zero as the value of the input x deviates from δ .

These two problems can be solved to a large degree with the use of the **n**logistic-sigmoid, which features: one, a tunable logistic growth-rate constant, such that the maximum gradient is neither too large nor too small; and two: a n -times occurring gradient map over the finite input-output space (universe).

III. NLOGISTIC-SIGMOID

Instead of the classic single sigmoid, a repeating sigmoid behaviour found in the motion-profile of ant-swarms can be emulated within a defined finite input-output universe specified by $[x_{\min}, x_{\max}]$ and $[y_{\min}, y_{\max}]$.

The specified finite input and output universe (space) is partitioned into n equal sub-spaces with n inflection points at $x = \delta_i$ leading to v_i sub-sigmoids, where $i = 1, \dots, n$. This transforms the classic logistic-sigmoid function to a sum of n shifted sigmoids each with a continuous gradient map over the surface of the input-output universe.

The interval spacing for each sub-sigmoid partition in the finite input and output universe can be defined respectively as (5) and (6).

$$\Delta_x = \frac{(x_{\max} - x_{\min})}{n} \quad (5)$$

$$\Delta_y = \frac{(y_{\max} - y_{\min})}{n} \quad (6)$$

A formal definition for the periodic odd function that results from the sum of shifted sigmoids, each having the same property, can then be provided.

Definition 1. The **n**logistic-sigmoid function, with odd output y and even output g , denoted as **n**lsig \pm : $\mathbb{R} \rightarrow \mathbb{R}$, where $n \in \mathbb{N}^+$ and $\lim_{x \rightarrow x_{\max}} y \rightarrow y_{\max}$, $\lim_{x \rightarrow x_{\min}} y \rightarrow y_{\min}$ is:

$$\mathbf{nlsig}\pm: y = \mathbf{f}(x) = \kappa_y + \sum_{i=1}^n v_i \quad (7)$$

$$g = \tau \sum_{i=1}^n v_i (\Delta_y - v_i) \quad (8)$$

where,

$$v_i = \frac{\Delta_y}{1 + e^{\pm u}}, u = \alpha(x - \delta_i) \quad (9)$$

$$\delta_i = \kappa_x + \Delta_x \left(i - \frac{1}{2} \right) \quad (10)$$

$$\alpha = \frac{2\lambda}{\Delta_x}, \quad \tau = \frac{\alpha}{\Delta_y} \quad (11)$$

and,

$$\kappa_x = x_{\min}, \kappa_y = y_{\min}, \lambda = 6.$$

The boundary (limit) values of the input-output universe are defined as:

$$y_{\max} = (1 - \xi) y_{\max}, \quad y_{\min} = (1 - \xi) y_{\min} \quad (12)$$

$$x_{\max} = (1 - \xi) x_{\max}, \quad x_{\min} = (1 - \xi) x_{\min} \quad (13)$$

where

$$\xi = \xi/c, \quad -c \leq \xi \leq c \quad (14)$$

and

$$c = 100 \quad \text{and} \quad \xi = 0 \text{ (default)} \quad (15)$$

with $\xi, c \in \mathbb{N}^+$, and $x, y, g, v, \alpha, \delta, \tau \in \mathbb{R}$.

The midpoint of the input-output limits is (\bar{x}, \bar{y}) .

$$\bar{x} = \frac{x_{\max} + x_{\min}}{2} \quad (16)$$

$$\bar{y} = \frac{y_{\max} + y_{\min}}{2} \quad (17)$$

There is no central inflection point when n is even. The central inflection point $\bar{\delta}$, when n is odd is equivalent to \bar{x} .

$$\bar{\delta} = \frac{1}{n} \sum_{i=1}^n \delta_i = \bar{x} \quad (18)$$

The parameter n defines the number of sub-sigmoids in the function, τ is the derivative constant, v_i is partial output representing the i th sub-sigmoid, u is the natural exponential input, and ξ is the limit damper constant.

From the definitions in (16) and (17), it is also straightforward to see that, to ensure the curve is symmetric at a central midpoint of $\bar{\delta} = 0$, then the minimum limit must always be set as $x_{\min} = -x_{\max}$ and $y_{\min} = -y_{\max}$.

The output shape of the **n**logistic-sigmoid function is illustrated for an arbitrary finite input-output universe $[-10, 10]$ in Fig. 1-3.

The logistic input-output approximation behaviour of the **n**logistic-sigmoid function in its finite universe is dependent on λ , the logistic growth-rate constant. λ controls how the behaviour of the output and also how the maximum gradient will repeat itself n times at every $x = \delta_i$, with the gradient value diminishing to zero only at the maximum and minimum limits of the input-output interval. This is illustrated in Fig. 2. The best input-output sigmoidal approximation occurs when $\lambda = 6$.

It can be shown that the value of the maximum gradient \bar{g} is proportional to the value of λ .

Proof. To start with, we note that the sigmoid shape repeats itself n -times in the input-output universe. Since, this is true, then without any loss of generality, we can assume $n = 1$. The derivative becomes:

$$g = \tau v (\Delta_y - v)$$

where

$$v = y - y_{\min}, \quad \Delta_y = y_{\max} - y_{\min}$$

At the interval boundaries or limits, when $y = y_{\max}$ or $y = y_{\min}$, then $g = 0$.

Also, at the inflection-point (mid-point), when $x = \bar{\delta}$, the output value is $y = (y_{\max} + y_{\min})/2$, then $g = (\lambda \Delta_y) / (2 \Delta_x)$.

For a symmetric map, centered at zero, with $x_{\max} \equiv y_{\max}$ and $x_{\min} \equiv y_{\min}$, we have $\Delta_x = \Delta_y$, and so $g = \lambda/2$.

Since $\lambda = 6$, the value of the derivative at the midpoint becomes $g = 3$. Therefore, in one line

$$\bar{g} = 0.5 \lambda \frac{\Delta_y}{\Delta_x} = 0.5 \lambda \frac{y_{\max}}{x_{\max}} = 0.5 \lambda = 3$$

It follows that, if $n > 1$, then, the maximum gradient will occur at each $x = \delta_i$, which represent the centre of each sub-sigmoid. Also, as $\lambda = 6$, the maximum gradient \bar{g} is always 3 at $x = \delta_i$. This completes the proof. \square

Therefore, with the definition of the **n**logistic-sigmoid function, gradients do not vanish except at the boundary of the maximum or minimum of the input-output universe. This is visually illustrated in Fig. 3a. Consequently, to a large extent, because of the way the gradient is controlled and repeated over the input-output map, the frequent occurrence of vanishing gradients in the network's gradient flow and local gradient will be far reduced, compared to the classic sigmoid use-case.

Since this function definition is the intended contribution of this paper, we leave the empirical evaluation and comparison of its performance to the classic sigmoid variants and rectified-linear unit variants on benchmark ANN data-sets as future work.

Further, we note that as n increases in the **n**logistic-sigmoid function, approximately linear regions around the inflection points become more evident as shown in Fig. 3b. This behaviour is influenced by the logistic growth-rate constant λ , and offers the advantage of better function approximation as discussed in [23]. Lyapunov stability is also guaranteed by the **n**logistic-sigmoid function under certain conditions for RNNs as shown for shifted sigmoids in [24], [38].

Finally, we note that compared to rectified linear-units, and the classic logistic-sigmoids, the main inherent drawback of the proposed function is the increased arithmetic and exponential operations as the n parameter is increased. Notwithstanding this short-coming, satisfactory computational-speed and accuracy can be obtained from computing the natural exponential term by using a combination of software computing techniques: ones-normalization, bit-manipulation and exponentiation-by-squaring.

IV. CONCLUSIONS

The **n**logistic-sigmoid function which extends the classic sigmoid function to a function of n sigmoids over a defined finite input-output map was contributed in this brief. It was analytically shown by definition and also by visual illustration that this function inherently overcomes to a large extent the famous vanishing-gradient problem of sigmoid functions. Apart from the intended popular use as a activation function and reward function in deep neural network architectures, the **n**logistic-sigmoid will also find suitable application as a fuzzy membership function, a nonlinear estimator, a smooth control law, a signal limiter, and as a nonlinear filter.

REFERENCES

- [1] V. Sze, Y.-H. Chen, T.-J. Yang, and J. S. Emer, "Efficient Processing of Deep Neural Networks: A Tutorial and Survey," *Proceedings of the IEEE*, vol. 105, no. 12, pp. 2295–2329, Dec. 2017.
- [2] P. Kim, *MATLAB Deep Learning: With Machine Learning, Neural Networks and Artificial Intelligence*. Berkeley, CA: Apress, 2017.
- [3] Y. LeCun, L. Bottou, G. B. Orr, and K. R. Müller, "Efficient BackProp," in *Neural Networks: Tricks of the Trade*, ser. Lecture Notes in Computer Science, G. B. Orr and K.-R. Müller, Eds. Berlin, Heidelberg: Springer Berlin Heidelberg, 1998, pp. 9–50.

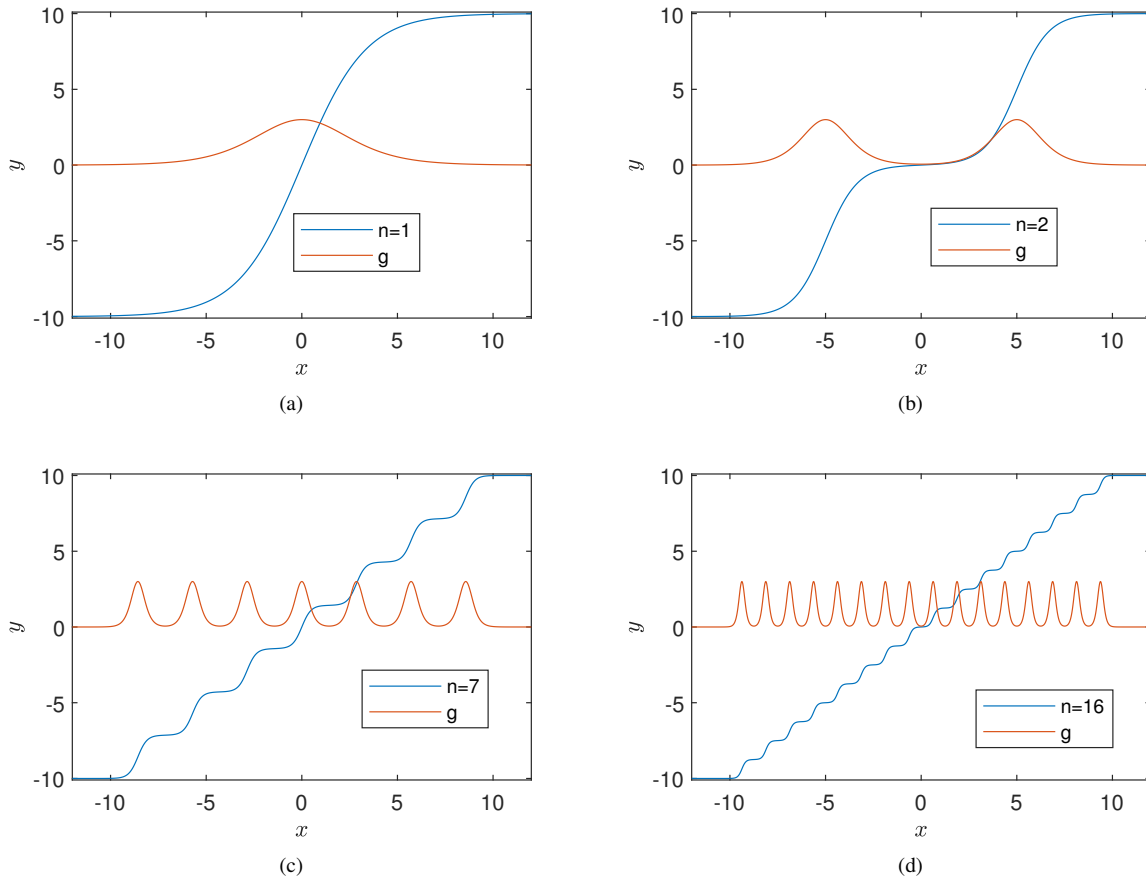


Fig. 2. Output and Gradient Plot of the **nlogistic-sigmoid**: $n = 1$ in Fig. (2a), $n = 2$ in Fig. (2b), $n = 7$ in Fig. (2c), and $n = 16$ in Fig. (2d).

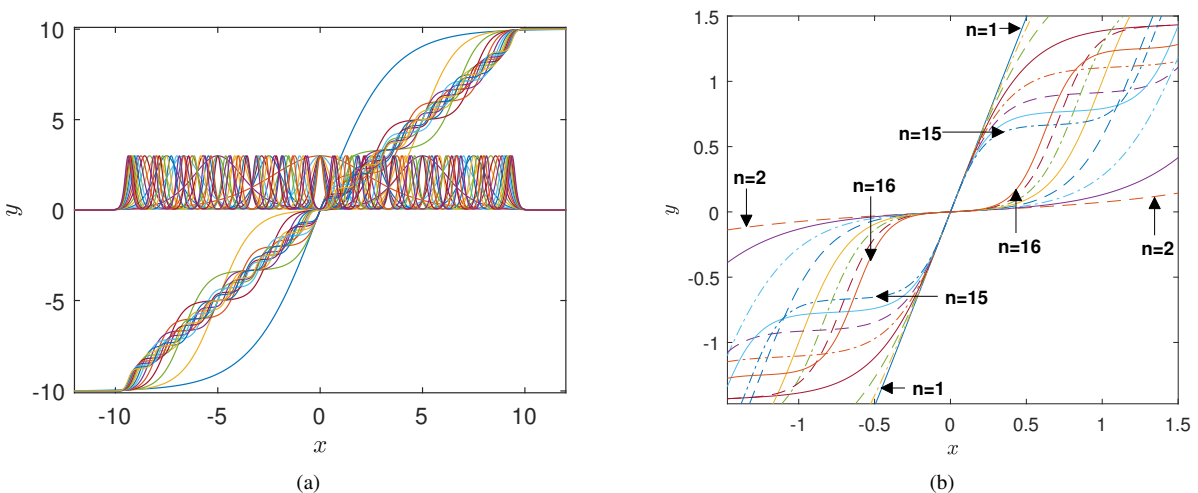


Fig. 3. Full plot of the **nlogistic-sigmoid** for $n = 1$ to 16. Fig. (3b) shows a detailed zoomed view of the output.

- [4] T. G. Tan, J. Teo, and P. Anthony, "A comparative investigation of non-linear activation functions in neural controllers for search-based game AI engineering," *Artificial Intelligence Review*, vol. 41, no. 1, pp. 1–25, Jan. 2014.
- [5] J. Han and C. Moraga, "The influence of the sigmoid function parameters on the speed of backpropagation learning," in *From Natural to Artificial Neural Computation*, ser. Lecture Notes in Computer Science, J. Mira and F. Sandoval, Eds. Berlin, Heidelberg: Springer, 1995, pp. 195–201.
- [6] P. Werbos, "Backpropagation through time: What it does and how to do it," *Proceedings of the IEEE*, vol. 78, no. 10, pp. 1550–1560, Oct. 1990.
- [7] J. P. Chibole, "Performance Analysis of the Sigmoid and Fibonacci Activation Functions in NGA Architecture for a Generalized Independent Component Analysis," 2017.
- [8] O. Omidvar and D. L. Elliott, *Neural Systems for Control*, 1st ed. Academic Press, 1997.

- [9] S. Lipovetsky, "Double logistic curve in regression modeling," *Journal of Applied Statistics*, vol. 37, no. 11, pp. 1785–1793, Nov. 2010.
- [10] L. M. McDowall and R. A. L. Dampney, "Calculation of threshold and saturation points of sigmoidal baroreflex function curves," *American Journal of Physiology-Heart and Circulatory Physiology*, vol. 291, no. 4, pp. H2003–H2007, Oct. 2006.
- [11] A. Perna, B. Granovskiy, S. Garnier, S. C. Nicolis, M. Labédan, G. Theraulaz, V. Fourcassié, and D. J. T. Sumpter, "Individual Rules for Trail Pattern Formation in Argentine Ants (*Linepithema humile*)," *PLOS Computational Biology*, vol. 8, no. 7, p. e1002592, Jul. 2012.
- [12] W.-K. Chen, *Feedback, Nonlinear, and Distributed Circuits*. CRC Press, Oct. 2018.
- [13] P. Vas, *Artificial-Intelligence-Based Electrical Machines and Drives: Application of Fuzzy, Neural, Fuzzy-Neural, and Genetic-Algorithm-Based Techniques*, ser. Monographs in Electrical and Electronic Engineering. Oxford, New York: Oxford University Press, Jan. 1999.
- [14] J. Pineda de Gyvez, "Hardware Implementation of a Desktop Supercomputer for High Performance Image Processing. Time Multiplexed Color Image Processing Based on a VLSI Cellular Neural Network with Cell-State Outputs," Texas A and M University College Station Dept Of Electrical Engineering, Technical, 1994.
- [15] J. D. Rairan, "Robot Path Optimization Based on a Reference Model and Sigmoid Functions," *International Journal of Advanced Robotic Systems*, vol. 12, no. 3, p. 19, Mar. 2015.
- [16] M. A. Mansor and S. Sathasivam, "Performance analysis of activation function in higher order logic programming," *AIP Conference Proceedings*, vol. 1750, no. 1, p. 030007, Jun. 2016.
- [17] D. Mohammad, A. H. Elshafie, J. Othman, O. A. Karim, and M. Sharifah, "Comparison of artificial neural network transfer functions abilities to simulate extreme runoff data," *International Proceedings of Chemical, Biological and Environmental Engineering (IPCBE)*, vol. 33, pp. 39–44, 2012.
- [18] M. D. Klimek and M. Perelstein, "Neural Network-Based Approach to Phase Space Integration," *arXiv:1810.11509 [hep-ex, physics:hep-ph, physics:physics, stat]*, Oct. 2018.
- [19] M. A. Sartin and A. C. R. da Silva, "Approximation of hyperbolic tangent activation function using hybrid methods," in *2013 8th International Workshop on Reconfigurable and Communication-Centric Systems-on-Chip (ReCoSoC)*, Jul. 2013, pp. 1–6.
- [20] Che-Wei Lin and Jeen-Shing Wang, "A digital circuit design of hyperbolic tangent sigmoid function for neural networks," in *2008 IEEE International Symposium on Circuits and Systems*, May 2008, pp. 856–859.
- [21] L. Paralı, A. Sari, U. Kılıç, Ö. Şahin, and J. Pěchoušek, "The artificial neural network modelling of the piezoelectric actuator vibrations using laser displacement sensor," *Journal of Electrical Engineering*, vol. 68, no. 5, pp. 371–377, Sep. 2017.
- [22] B. Zamanlooy and M. Mirhassani, "Efficient VLSI Implementation of Neural Networks With Hyperbolic Tangent Activation Function," *IEEE Transactions on Very Large Scale Integration (VLSI) Systems*, vol. 22, no. 1, pp. 39–48, Jan. 2014.
- [23] I. Ohn and Y. Kim, "Smooth Function Approximation by Deep Neural Networks with General Activation Functions," *Entropy*, vol. 21, no. 7, p. 627, Jul. 2019.
- [24] M. Mostafa, W. G. Teich, and J. Lindner, "Approximation of activation functions for vector equalization based on recurrent neural networks," in *2014 8th International Symposium on Turbo Codes and Iterative Information Processing (ISTC)*, Aug. 2014, pp. 52–56.
- [25] S. Hochreiter and J. Schmidhuber, "Long Short-Term Memory," *Neural Computation*, vol. 9, no. 8, pp. 1735–1780, Nov. 1997.
- [26] S. Kong and M. Takatsuka, "Hexpo: A vanishing-proof activation function," in *2017 International Joint Conference on Neural Networks (IJCNN)*. Anchorage, AK, USA: IEEE, May 2017, pp. 2562–2567.
- [27] J. Schmidhuber, "Deep learning in neural networks: An overview," *Neural Networks*, vol. 61, pp. 85–117, Jan. 2015.
- [28] B. Carlile, G. Delamarter, P. Kinney, A. Marti, and B. Whitney, "Improving Deep Learning by Inverse Square Root Linear Units (ISRLUs)," *arXiv:1710.09967 [cs]*, Oct. 2017.
- [29] D. L. Elliott and D. L. Elliott, *A Better Activation Function for Artificial Neural Networks*, 1993.
- [30] X. Jin, C. Xu, J. Feng, Y. Wei, J. Xiong, and S. Yan, "Deep Learning with S-shaped Rectified Linear Activation Units," *arXiv:1512.07030 [cs]*, Dec. 2015.
- [31] I. J. Goodfellow, D. Warde-Farley, M. Mirza, A. Courville, and Y. Bengio, "Maxout Networks," *arXiv:1302.4389 [cs, stat]*, Sep. 2013.
- [32] M. S. Gashler and S. C. Ashmore, "Training Deep Fourier Neural Networks To Fit Time-Series Data," *arXiv:1405.2262 [cs]*, May 2014.
- [33] C. Nwankpa, W. Ijomah, A. Gachagan, and S. Marshall, "Activation Functions: Comparison of trends in Practice and Research for Deep Learning," *arXiv:1811.03378 [cs]*, Nov. 2018.
- [34] N. G. Timmons and A. Rice, "Approximating Activation Functions," *arXiv:2001.06370 [cs, stat]*, Jan. 2020.
- [35] K. Greff, R. K. Srivastava, J. Koutník, B. R. Steunebrink, and J. Schmidhuber, "LSTM: A Search Space Odyssey," *IEEE Transactions on Neural Networks and Learning Systems*, vol. 28, no. 10, pp. 2222–2232, Oct. 2017.
- [36] J.-M. Muller, "Elementary Functions and Approximate Computing," *Proceedings of the IEEE*, pp. 1–14, 2020.
- [37] O. Somefun, "https://github.com/somefunAgba/nlogisticsigmoid," Jul. 2020.
- [38] M. Mostafa, W. G. Teich, and J. Lindner, "Local stability analysis of discrete-time, continuous-state, complex-valued recurrent neural networks with inner state feedback," *IEEE Transactions on Neural Networks and Learning Systems*, vol. 25, no. 4, pp. 830–836, 2014.